Enhanced glycoprotein production in HEK-293 cells expressing pyruvate carboxylase

Henry, Olivier; Durocher, Yves

Publisher's version / Version de l'éditeur:
https://doi.org/10.1016/j.ymben.2011.05.004
Metabolic Engineering, pp. 1-9, 2011-12-30

Metabolic Engineering ▮ (▮▮▮▮) ▮▮▮–▮▮▮

Contents lists available at ScienceDirect

Metabolic Engineering

journal homepage: www.elsevier.com/locate/ymben

Enhanced glycoprotein production in HEK-293 cells expressing pyruvate carboxylase

Olivier Henry [a,*], Yves Durocher [b]

[a] Département de Génie Chimique, École Polytechnique de Montréal, C.P. 6079, Succ. Centre-ville, Montréal, Québec, Canada H3C 3A7
[b] National Research Council Canada, Biotechnology Research Institute, 6100 Royalmount Avenue, Montréal, Québec, Canada H4P 2R2

ARTICLE INFO

Article history:
Received 23 February 2011
Received in revised form
26 April 2011
Accepted 13 May 2011

Keywords:
HEK-293 cells
Recombinant interferon
Pyruvate carboxylase
^{13}C-metabolic flux analysis

ABSTRACT

There is an imperative need for expression systems allowing the efficient and robust manufacturing of high quality glycoproteins. In the present work, HEK-293 cells stably expressing interferon-α2b were further engineered with the insertion of the yeast pyruvate carboxylase 2 gene. In batch cultures, marked reductions in lactate and ammonia production were observed compared to the parental cell clone. Although the maximum specific growth rate remained unchanged, the altered metabolism led to a 2-fold increase in maximum cell density and 33% increase in the integral of viable cell concentration and interferon production yield. The underlying metabolic changes were further investigated using various ^{13}C-labeled substrates and measuring the resulting lactate mass isotopomer distributions. Simultaneous metabolite and isotopomer balancing allowed the accurate determination of key intracellular fluxes. Such detailed and quantitative knowledge about the central carbon metabolism of the cells is instrumental to further support the development of high-yield fed-batch processes.

1. Introduction

HEK-293 cells are extensively used for the production of various viral vectors, including adenovirus (Kamen and Henry, 2004), adeno-associated virus (Durocher et al., 2007), retrovirus (Ghani et al., 2006) and lentivirus (Broussau et al., 2008). Due to their human origin, their ability to grow in serum-free suspension culture and their high transfectability, the HEK-293 cells also constitute an attractive platform for the transient or stable expression of recombinant proteins requiring proper post-translational modifications (Durocher and Butler, 2009; Durocher et al., 2002; Zhang et al., 2010). We have recently described the establishment of an HEK-293 cell clone (D9) with a stable expression of interferon-α2b (IFNα2b), allowing to reach product yields in excess of 200 mg/L in serum-free batch culture (Loignon et al., 2008). The purified product was shown to be O-glycosylated, heavily sialylated and biologically active. The efficient and cost-effective production of biotherapeutics in mammalian cell cultures requires the development of processes supporting high cell densities and high cell specific productivities (Durocher and Butler, 2009; Ng et al., 2007; Wurm, 2004). Thus, efforts are now being devoted to further increasing the yields of glycoprotein production by applying metabolic engineering approaches at both the process and cellular levels.

In mammalian cell cultures, cell density and product concentration are often low due to the accumulation of lactate and ammonia, the two major metabolic by-products of glucose and amino acids metabolism (Quek et al., 2009a). They are well known inhibitors of both cellular growth and productivity, with detrimental effects reported for lactate levels exceeding 20 mM and ammonia concentrations as low as 2–3 mM (Cruz et al., 2000; Glacken, 1986; Hassell et al., 1991; Omasa et al., 1992a; Ozturk et al., 1992). Moreover, these metabolites were shown to adversely affect product quality, most notably by altering the glycosylation pattern (Andersen and Goochee, 1995; Borys et al., 1994; Chen and Harcum, 2006; Gawlitzek et al., 1998; Grammatikos et al., 1998). Consequently, numerous strategies have been explored to reduce the build-up of these toxic metabolites with the goals of achieving high viable cell concentrations, extending culture time and improving product yield and quality.

At the process level, the apparent deregulation of glucose and glutamine uptake rates when these nutrients are present in excess has led to the implementation of controlled feeding strategies to maintain low but non-limiting levels of the main nutrient concentrations (Europa et al., 2000; Gambhir et al., 1999; Kurokawa et al., 1994; Lee et al., 2003; Ljunggren and Haggstrom, 1992, 1994; Omasa et al., 1992a, 1992b; Siegwart et al., 1999; Zhou et al., 1995). Such strategies have proven effective at reducing the overall yield of lactate on glucose, but require on-line monitoring of nutrient concentrations and automatic feed rate adjustment during the culture. Metabolic waste formation was also reduced through modifications of the medium composition, such as substituting glucose with galactose (Altamirano et al., 2000, 2004) or pyruvate (Genzel et al., 2005), glutamate (Hassell and Butler, 1990) or asparagine (Kurano et al., 1990) for glutamine, or through the addition of TCA intermediates in the culture medium (Omasa et al., 2009). While effectively reducing

* Corresponding author. Fax: +1 514 340 4159.
E-mail address: olivier.henry@polymtl.ca (O. Henry).

1096-7176/$ - see front matter © 2011 Elsevier Inc. All rights reserved.
doi:10.1016/j.ymben.2011.05.004

lactate or ammonia accumulation, these changes may also negatively impact on the growth and/or productivity of the cells. Finally, various separation techniques have also been explored for the in-situ selective removal of lactate and ammonia from the culture broth (Brose and van Eikeren, 1990; Chang et al., 1995; Nayve et al., 1991), but have not yet found widespread application.

At the cellular level, several host engineering approaches were proposed to design continuous cell lines with improved characteristics, such as enhanced secretary capacity (Peng et al., 2010) or more efficient nutrient utilization achieved through an alteration of their primary metabolism. A key early success was achieved with the insertion and amplification of the glutamine synthetase gene in CHO and myeloma cells, allowing growth in glutamine-free medium and thereby significantly reducing ammonia formation (Bebbington et al., 1992; Birch et al., 1994; Cockett et al., 1990). Partial disruption of the gene encoding lactate dehydrogenase A in hybridoma cells was also shown to lower the production of lactate, translating into an increase in cell concentration and antibody production (Chen et al., 2001). Another approach consisted of the expression of a yeast pyruvate carboxylase (PYC) gene in mammalian cells to compensate for the apparent lack of enzymatic activities linking glycolysis and the TCA cycle. This enzyme, catalyzing the anaplerotic conversion of pyruvate to oxaloacetate, is naturally present in mammalian cells, but several isotopic tracer studies revealed that pyruvate incorporation into the TCA mainly occurs via the pyruvate dehydrogenase reaction (Bonarius et al., 2001; Mancuso et al., 1994; Metallo et al., 2009). PYC expression was shown to have a profound effect on the metabolism of several relevant cell lines, including BHK-21 cells (Irani et al., 1999), HEK-293 cells (Elias et al., 2003) and CHO cells (Kim and Lee, 2007). All these studies have reported marked reductions in glucose uptake and lactate formation rates resulting from PYC expression. Interestingly, ammonia production was also inhibited, demonstrating the intricate link between glutamine and glucose metabolism. However, despite exhibiting a highly efficient nutrient utilization, these altered metabolisms yielded mixed results in term of cellular growth and productivity enhancements. Moreover, while $^{14}CO_2$ measurements have suggested an increase incorporation of glucose carbon into the TCA cycle resulting from the expression of the PYC gene (Irani et al., 1999), the actual pyruvate carboxylase flux has not been evaluated in these studies.

In this work, we have investigated the potential of expressing the PYC2 gene in HEK-293 cells to enhance the production of recombinant IFNα2b. The cellular kinetics of the PYC-overexpressing cells in batch cultures were compared to the parental cell clone stably expressing the glycoprotein. To provide a detailed and quantitative description of the underlying physiological changes observed, we have conducted a ^{13}C-metabolic flux analysis on the two cell clones. To this end, cells were grown with various labeled substrates and the resulting mass isotopomer distributions of lactate were measured by LC-MS. Simultaneous metabolite and isotopomer balancing was then used to estimate the intracellular flux distribution in both the parental and the PYC-expressing cell lines. Such metabolic characterization is needed for the rational design of improved medium formulation and feeding strategies (Xie and Wang, 1996).

2. Materials and methods

2.1. Cell lines, medium and culture conditions

The HEK293-IFN clone D9 (293-D9) stably producing interferon-α2b was established from the 293-6E cell line constitutively expressing an EBNA1 protein of the Epstein–Barr virus, as previously described (Loignon et al., 2008). The HEK293-IFN-PYC clone F5 (293-F5) was obtained by transfection of the 293-D9 cell line with the pCEP5a vector (Durocher et al., 2002) encoding the yeast pyruvate carboxylase 2 gene (GeneID: 852519; Elias et al., 2003). Stable transfectants were selected using 10 μg/ml of hygromycin in Freestyle 293 medium (Invitrogen) and clones derived from single colonies were amplified and screened for PYC2 expression by western blot using HRP-conjugated streptavidin (Sigma). The clone F5 was selected based on PYC2 expression level and stability in the absence of hygromycin. The pool of transfected cells from which this clone was isolated was also characterized in terms of cellular growth, nutrient consumption, waste metabolite production and interferon yield. Since the F5 clone and the pool of transfected cells exhibited comparable kinetics rates, clonal variation effects were ruled out as a determinant factor for the differences observed in our study. Cells were grown in glucose-free LC-SFM medium (Invitrogen) supplemented with 1% BSA, 25 mM glucose and 4 mM glutamine. Batch cultures were performed in 125 mL shaker flasks (Corning) at an initial working volume of 20 mL. Cultures were inoculated at a cell concentration of 0.2×10^6 cells/mL and were grown at 37 °C and 5% CO_2 under constant agitation (120 rpm). Isotopic tracer studies were conducted using 1-^{13}C, 6-^{13}C, U-^{13}C glucose and U-^{13}C glutamine (Cambridge Isotopes), all at 99% purity. The cultures were carried out in parallel in 50 mL spin-tubes (Sartorius) at a working volume of 4 mL and were operated in a semi-continuous mode, whereby a fraction of spent culture volume was replaced with fresh medium on a daily basis. Upon reaching pseudo-steady cell and nutrient concentrations, cultures were centrifuged and re-suspended in fresh medium containing the ^{13}C-enriched substrate and semi-continuous operation was continued for up to 5 days. This mode of operation was chosen over batch cultivation to ensure the attainment of isotopic steady state conditions by maintaining the cells under balanced exponential growth conditions (Deshpande et al., 2009), while alleviating the need for a more complex small-scale chemostat setup (Henry et al., 2008).

2.2. Analytical methods

Total cell concentration was determined using a haemocytometer (Hausser Scientific, Horshaw, PA) and cell viability was assessed by dye exclusion method using erythrosine B. Samples taken from the cultures were frozen at −80 °C until ready for analysis. Glucose, lactate and ammonia were measured with a Biolyzer instrument (Kodak, New Haven, Connecticut). Amino acids in the culture supernatant were quantified by the AccQ-tag method (Pham et al., 2003). The interferon was measured by an ELISA assay as described in Loignon et al. (2008). Lactate in the supernatant was separated by an HPLC system (Dionex Canada, Oakville, ON) using an Ion Pac AS11-HC column equipped with an AG11 pre-column as previously described (Lioussanne et al., 2008). The mass isotopomer distribution of lactate was determined by recording electrospray ionization (ESI) mass spectra in the negative ion mode using a Micromass ZQ detector (Waters, Milford, MA). The medium sample was infused with a syringe pump at a flow rate of 20 μL/min. The operating conditions of the mass spectrometer were as followed: capillary voltage, 3.0 kV; cone voltage, −23 V; extractor voltage, −3 V and RF lens voltage, −0.2 V. The source temperature was 110 °C, the desolvation temperature was 300 °C and nitrogen gas was used as a nebulizer and drying gas.

2.3. Intracellular flux calculation

The reaction network employed in this study was adapted from a comprehensive metabolic model previously established for HEK-293 cells (Henry et al., 2005; Nadeau et al., 2002). The model considers the main pathways from the central carbon metabolism including glycolysis, the pentose phosphate pathway, the TCA cycle, anaplerotic

Please cite this article as: Henry, O., Durocher, Y., Enhanced glycoprotein production in HEK-293 cells expressing pyruvate carboxylase. Metab. Eng. (2011), doi:10.1016/j.ymben.2011.05.004

reactions and the catabolism of 18 amino acids. The biosynthetic rates were calculated assuming a constant average cellular composition (on a dry weight basis) in lipids, DNA/RNA and proteins, as previously measured for HEK-293 cells (Nadeau et al., 2002). Intracellular flux distributions were evaluated by simultaneous metabolite and isotopomer balancing using the biochemical reactions and the corresponding atom transitions listed in Table A1 (Appendix A1). As none of the exchange fluxes in our model was observable with the labeling data at hand, all reactions were treated as unidirectional. Metabolic compartmentation was not taken into account and, therefore, cytosolic pools of oxaloacetate, malate and pyruvate, which can be transported across the mitochondrial membrane, were assumed to have the same labeling distribution as their mitochondrial counterparts (Bonarius et al., 2001; Hofmann et al., 2008; Metallo et al., 2009). The metabolic model consisted of 25 biochemical reactions, of which 10 were directly calculable from measurements, and 13 balanceable metabolites. The lactate isotopomer distributions obtained from the four labeled substrates yielded 12 additional measurements. The unknown free fluxes were estimated by a non-linear fitting procedure to minimize the difference between experimental and simulated isotopomer data. For each cell clone, a single optimization was performed using mass distribution measurements from the four parallel cultures. Calculations were implemented and performed in the OpenFLUX software package (Quek et al., 2009b). The goodness of fit was assessed with a χ^2 test applied to the obtained minimal sum of squares of residuals and 95% confidence intervals for the fluxes were calculated according to the approach described by Antoniewicz et al. (2006).

3. Results

3.1. Cell growth and IFNα2β production in batch cultures

The parental (293-D9) and PYC-overexpressing (293-F5) cells were grown in batch mode and the resulting cell density profiles are shown in Fig. 1A. The 293-F5 cells reached a maximum cell concentration of about 3×10^6 cells/mL, a nearly 2-fold increase compared with the parental cells. This increase was mainly due to a prolonged exponential growth phase, as the maximum specific growth rates were fairly similar for the two cell lines (0.022 and 0.020 h^{-1} for the D9 and the F5 clones, respectively). Upon reaching their maximum in concentration at 150 h, the 293-F5 cells exhibited a sharp decrease in cell viability, likely as a result of a key nutrient depletion. In contrast, this decrease was less pronounced during the decline phase in the case of the parental cells. After 215 h of cultivation time, the integral of viable cell (IVC) was nonetheless 33% greater for the PYC-expressing cells. The corresponding glucose, lactate and ammonia concentration profiles are depicted in Fig. 1B–D. As expected, the insertion of the PYC2 gene led to a marked reduction in lactate formation. The 293-F5 cells were even shown to experience a metabolic shift characterized by the consumption of lactate during the period corresponding to the late exponential phase. Concomitant with the reduction in lactate formation, the final ammonia concentration was also reduced by a factor of 2. An analysis of amino acids utilization indicated that the consumption of glutamine and the production of glutamate and proline were all significantly reduced (Fig. 2). Interestingly, unlike for the parental cell clone, there was a net production of asparagine by the 293-F5 cells, presumably as a result of an increased flux from pyruvate to oxaloacetate, the latter being the biosynthetic precursor for this amino acid. As shown in Fig. 3, the altered metabolism led to an increase in volumetric productivity, as the PYC-expressing cells yielded a maximum interferon concentration of 80 mg/L, compared with 60 mg/L for the parental cells. This increase in product concentration was solely attributable to the increase in biomass, since the cell specific productivity (calculated with respect to the integral of viable cell, Luan et al., 1987) remained unchanged at circa 0.2 mg/10^9cells h for the two cell clones.

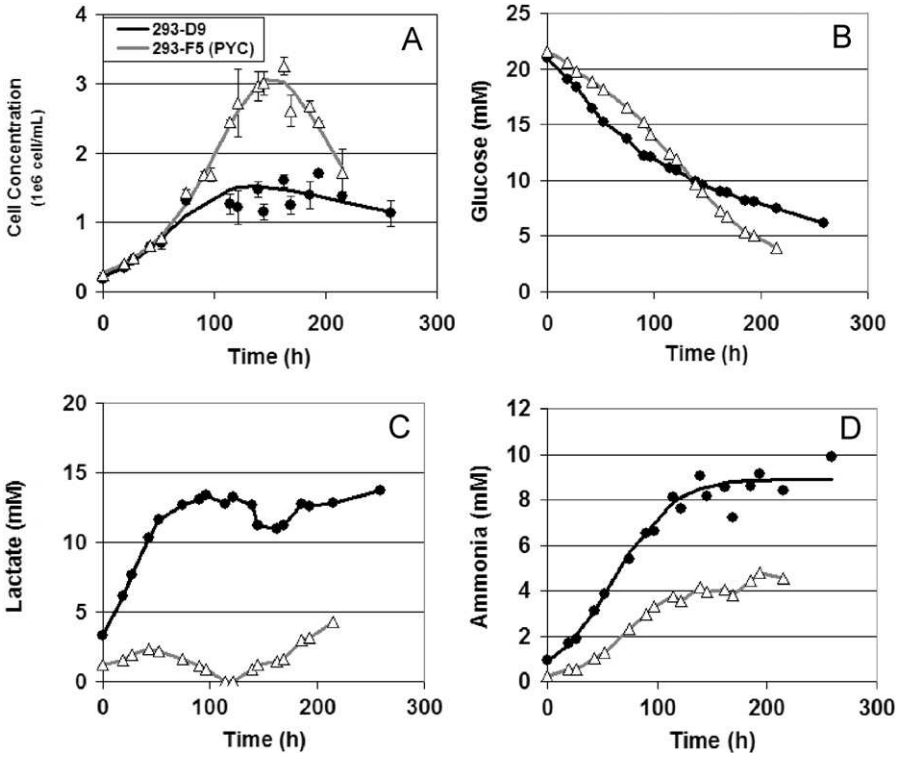

Fig. 1. Viable cell (A), glucose (B), lactate (C) and ammonia (D) concentrations profiles during batch cultivation of 293-D9 and 293-F5 cells.

Please cite this article as: Henry, O., Durocher, Y., Enhanced glycoprotein production in HEK-293 cells expressing pyruvate carboxylase. Metab. Eng. (2011), doi:10.1016/j.ymben.2011.05.004

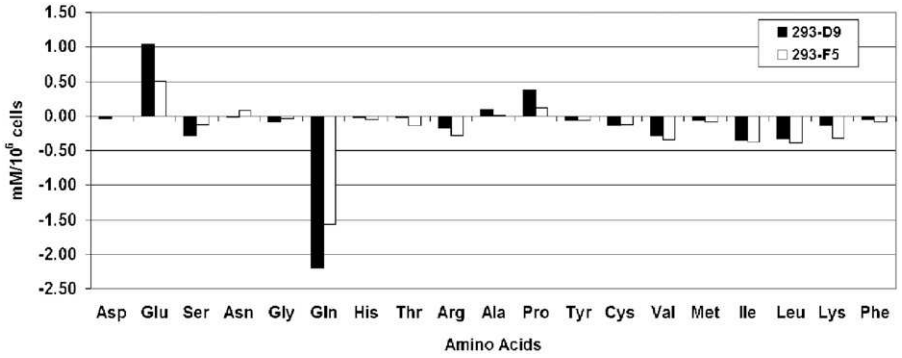

Fig. 2. Comparison of amino acids utilization by 293-D9 and 293-F5 cells in batch culture (from 0 to 162 h). Positive values indicate a net production.

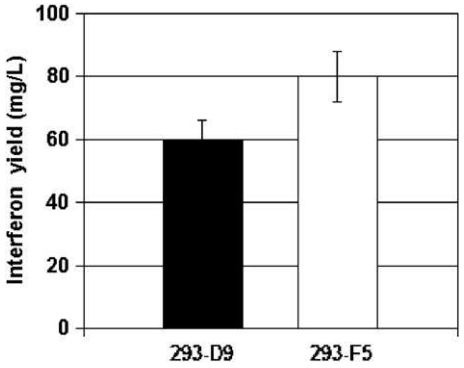

Fig. 3. Comparison of recombinant interferon yield between 293-D9 and 293-F5 cells in batch cultivation.

3.2. Cell kinetics and ^{13}C metabolic flux analysis in semi-continuous cultures

Semi-continuous cultures were performed to allow the determination of the cell specific consumption/production rates and the labeling distributions under metabolic and isotopic pseudo-steady state conditions. All semi-continuous cultures were maintained within the range of $0.7–1.2 \times 10^6$ cells/mL and at $>90\%$ viability. From the fraction of broth volume exchanged to maintain pseudo-constant conditions, the growth rates were determined to be 0.016 and 0.014 h^{-1} for the D9 and F5 cell lines, respectively. These values were slightly lower than those observed in batch, presumably due to the different cultivation systems employed (shake flasks vs spintubes). The experimentally determined average cell specific nutrient uptake and metabolite production rates are reported in Table 1. At pseudo-steady-state, glucose consumption was approximately reduced by a factor of 2 and lactate production by a factor of 6 for the 293-F5 cells. It is noteworthy that the molar ratio of lactate production to glucose consumption for the PYC-expressing cells was only 0.3, which is noticeably smaller than values commonly reported for mammalian cells (typically in the range of 1–2). While the uptake rate of glutamine was reduced by 15%, the consumption rates of most other essential amino acids were slightly enhanced. However, for both cell lines, the specific consumption rates of amino acids remained comparatively small relative to the glucose uptake rate.

Fig. 4 shows the resulting lactate mass distributions obtained when the two cell lines were grown using various ^{13}C-labeled substrates. The standard deviations of the individual mass abundance measurements were in the range of 1–2%. As expected, the distinct phenotypes of the two cell clones were reflected in the different labeling patterns of lactate obtained. Differences in the mass distributions corresponding to 1-^{13}C and 6-^{13}C glucose are directly indicative of pentose phosphate pathway activity, since the 1-C position of glucose-6-phosphate is released as carbon dioxide by the 6-phosphogluconate-dehydrogenase reaction. Flux through the pentose phosphate pathway was therefore greater in the case of the parental cells. The mass distributions corresponding to uniformly labeled substrates also revealed that the vast majority of lactate originated from the glucose metabolized directly through glycolysis. Although comparatively small, the presence of non-labeled or partially labeled lactate indicated the contribution of amino acids and/or the presence of pyruvate recycling from the TCA cycles. In order to get a more quantitative description of the underlying physiological differences, these labeling distributions and the measured uptake/consumption rates were used as inputs to the metabolic model for evaluating the intracellular fluxes in both cell lines. Fig. 4 shows the calculated (fit) values in comparison with the experimental lactate mass distributions. The variance weighted sum squares of the residuals were 10.5 and 16.9 for the D9 and F5 cell clones, respectively. Despite minor discrepancies with the experimental results, the model fits were statistically acceptable, since a χ^2 test (with 10 degrees of freedom) for goodness of fit yields a maximum allowable objective value of 18.3 at the 95% confidence

Table 1
Measured specific uptake (negative values) and production rates (positive values) during semi-continuous cultures. Errors are standard deviations from a minimum of 3 pseudo-steady state measurements.

Nutrient/metabolite	Specific uptake or production rate (pmol/cell d)	
	293-D9	293-F5
Glucose	-3.22 ± 0.18	-1.75 ± 0.09
Lactate	3.05 ± 0.15	0.53 ± 0.03
Aspartate	0.00 ± 0.01	0.01 ± 0.01
Glutamate	0.14 ± 0.01	0.09 ± 0.01
Serine	-0.07 ± 0.01	-0.07 ± 0.01
Asparagine	0.00 ± 0.01	0.06 ± 0.01
Glycine	0.02 ± 0.01	0.02 ± 0.01
Glutamine	-0.70 ± 0.07	-0.59 ± 0.06
Histidine	-0.01 ± 0.01	-0.02 ± 0.01
Threonine	-0.01 ± 0.01	-0.04 ± 0.01
Arginine	-0.07 ± 0.01	-0.09 ± 0.01
Alanine	0.07 ± 0.01	0.02 ± 0.01
Proline	0.11 ± 0.01	0.13 ± 0.01
Tyrosine	-0.02 ± 0.01	-0.03 ± 0.01
Cysteine	-0.03 ± 0.01	-0.05 ± 0.01
Valine	-0.08 ± 0.01	-0.13 ± 0.01
Methionine	-0.02 ± 0.01	-0.03 ± 0.01
Isoleucine	-0.11 ± 0.01	-0.17 ± 0.02
Leucine	-0.12 ± 0.01	-0.17 ± 0.02
Lysine	-0.06 ± 0.01	-0.10 ± 0.01
Phenylalanine	-0.02 ± 0.01	-0.03 ± 0.01

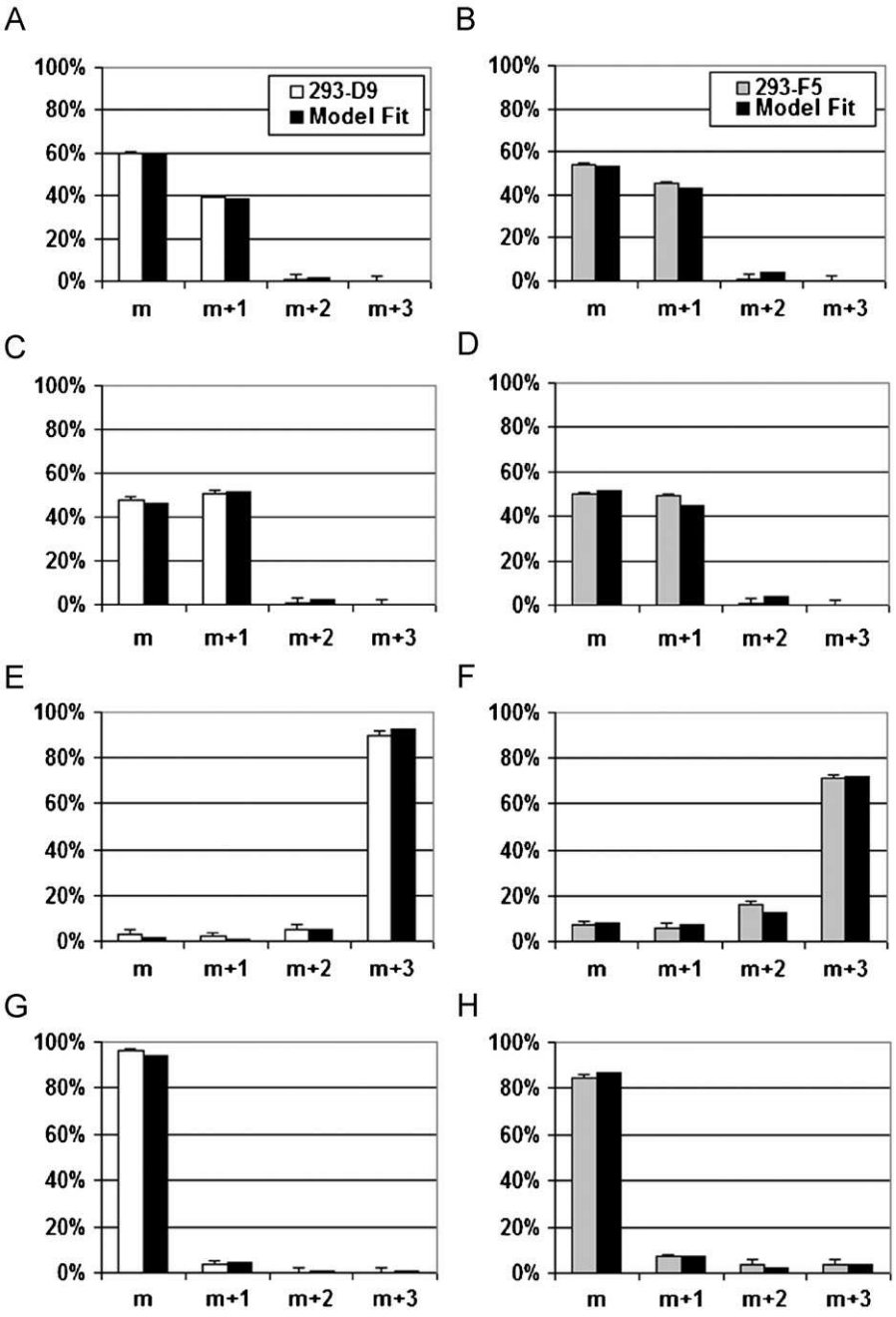

Fig. 4. Experimentally determined and simulated lactate mass isotopomer distributions in semi-continuous cultures grown with 1-^{13}C glucose (A, B), 6-^{13}C glucose (C, D), U-^{13}C glucose (E, F) and U-^{13}C glutamine (G, H). White and gray bars indicate the mass distributions determined by LC/MS for the 293-D9 and 293-F5 cells, respectively. The black bars represent the optimally fitted mass isotopomer distributions. m+i denotes the fractional abundance of the mass isotopomer containing i ^{13}C-atoms.

level. The average deviations between fitted and measured mass isotopomer data were 1.1% and 1.6%, and normal probability plots of the residuals were verified to be linear. The calculated intracellular flux distributions for both cell clones are shown in Fig. 5. To better assess the significance of observed differences, the corresponding 95% confidence intervals are reported in Table 2.

4. Discussion

HEK-293 cells modified to express the PYC2 gene exhibited a more efficient metabolism, characterized by marked reductions in glucose uptake, glutamine consumption, lactate production and ammonia formation. Compared with the parental cells, we observed a notable increase in the maximum cell density that translated into an increase in final product concentration during batch cultivation. The significant decrease in waste metabolite formation undoubtedly delays the acidification of the culture medium and may explain, at least in part, the higher maximum cell concentration achieved. However, the maximum specific growth rate and the cell specific productivity remained unchanged. In contrast to our results, expression of PYC in hGM-CSF producing CHO-K1 cells resulted in a lower maximum cell concentration, a reduced growth rate, a prolonged culture time and a two-fold increase in cell specific productivity (Fogolin et al., 2004). In the case of BHK21 cells, no noticeable effect

Please cite this article as: Henry, O., Durocher, Y., Enhanced glycoprotein production in HEK-293 cells expressing pyruvate carboxylase. Metab. Eng. (2011), doi:10.1016/j.ymben.2011.05.004

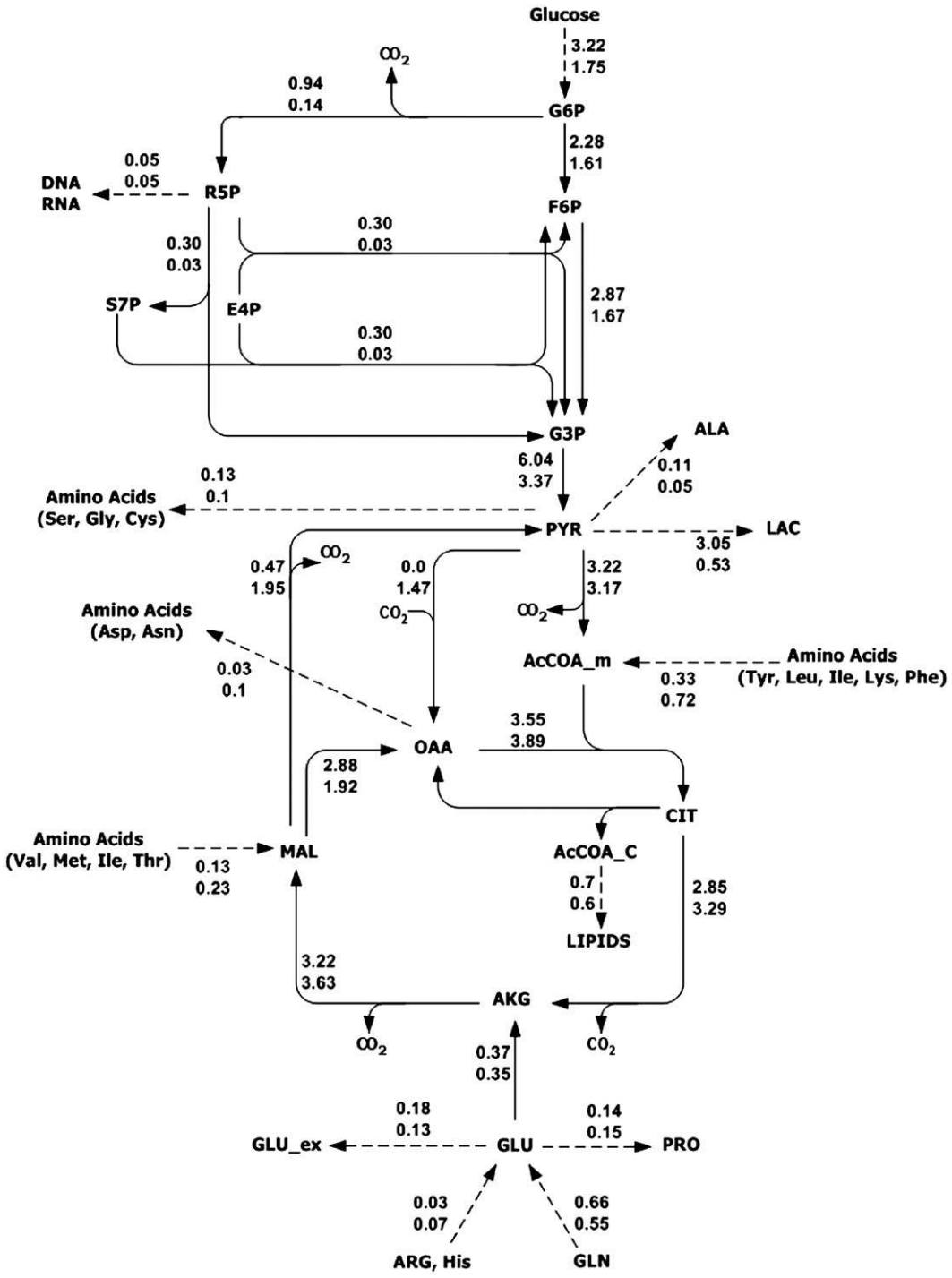

Fig. 5. Intracellular fluxes for 293-D9 (upper values) and 293-F5 (bottom values) cells. All fluxes are expressed in pmol/cell · d. Dashed lines indicate fluxes that were directly calculable from external rates and the cellular composition. Solid lines indicate intracellular fluxes that were estimated with the labeling data.

on the cell growth rate and maximum cell density in batch was observed (Irani et al., 1999), but culture viability was prolonged for three days. The cell specific productivity of recombinant human EPO was identical in PYC-expressing and control cells in perfusion cultures under non-limiting substrate conditions (Irani et al., 2002). Taken together, these results and our data indicate that the level and effects of PYC expression on cellular growth and productivity are likely both cell-type and process dependent. It should be noted that the interferon yields obtained in the current study are lower than those previously reported for the HEK-293 D9 clone (200 mg/L) (Loignon et al., 2008). However, these higher yields were achieved using a more complex medium formulation and the addition of peptone (0.1% TN1). The choice for the medium employed in our study was dictated by the requirements for conducting isotopic tracer studies, i.e. a well characterized and glucose/glutamine-free medium. This nonetheless demonstrates the potential of improvement achievable through the rational design of medium composition meeting the specific requirements for cellular growth and/or productivity.

Please cite this article as: Henry, O., Durocher, Y., Enhanced glycoprotein production in HEK-293 cells expressing pyruvate carboxylase. Metab. Eng. (2011), doi:10.1016/j.ymben.2011.05.004

Table 2
95% confidence intervals for the intracellular fluxes (pmol/cell d).

Reaction	293-D9	293-F5
Glycolytic and pentose phosphate pathway fluxes		
G6P→F6P	[2.12–2.51]	[1.43–1.79]
G6P→R5P+CO_2	[0.79–1.03]	[0.05–0.27]
2R5P→S7P+G3P	[0.25–0.33]	[0.0–0.07]
R5P+E4P→F6P+G3P	[0.25–0.33]	[0.0–0.07]
S7P+G3P→F6P+E4P	[0.25–0.33]	[0.0–0.07]
F6P→2G3P	[2.71–3.06]	[1.55–1.79]
G3P→PYR	[5.80–6.39]	[3.16–3.59]
TCA cycle and malic enzyme fluxes		
PYR→ACCOA+CO_2	[2.70–3.74]	[2.91–3.44]
ACCOA+OAA→CIT	[3.02–4.08]	[3.58–4.22]
CIT→AKG+CO_2	[2.26–3.40]	[2.95–3.64]
AKG→MAL+CO_2	[2.60–3.79]	[3.09–4.04]
MAL→OAA	[2.16–3.43]	[0.86–2.19]
MAL→PYR+CO_2	[0.42–0.84]	[1.70–3.08]
PYR→MAL+CO_2	[0.0–0.40]	[1.19–2.63]

In order to shed more light on the underlying physiological changes observed between the two cell clones, we have conducted a comprehensive ^{13}C metabolic flux analysis study. It should be emphasized that the experimental measurements performed in our work (mass spectrometry analysis of extracellular lactate) did not allow to quantify compartmental differences. Since we assumed rapid isotopic equilibration of metabolites between the compartments via effective shuttle systems, the TCA flux estimates presented in Fig. 5 are thus average values encompassing both the cytosolic and mitochondrial network activities. The analysis revealed that, at the pyruvate branch point, the parental cells converted 51% of the pyruvate pool into acetyl-CoA via the pyruvate dehydrogenase, 48% to lactate via lactate dehydrogenase and the remaining fraction to amino acids (mainly alanine and glycine). Our data suggested little to no significant flux through the pyruvate carboxylase, confirming an observation made by previous studies on several mammalian cells in culture (Bonarius et al., 2001; Mancuso et al., 1994; Metallo et al., 2009). In contrast, the PYC-expressing cells converted 56% of the pyruvate into acetyl-CoA, 26% into oxaloacetate via the pyruvate carboxylase and only 9% into lactate. Despite these different split ratios, as the glucose uptake was also reduced, the actual flux of pyruvate to acetyl-CoA remained similar in both cell clones (approximately 3.2 pmol/cell d), potentially suggesting that this pathway is operating at maximum capacity. The TCA cycle fluxes from citrate to oxaloacetate appeared to be enhanced by 15%, mainly due to the increase in the uptake of some essential amino acids (tyrosine, leucine, isoleucine, lysine and phenylalanine), but there is an overlap in the confidence intervals associated with these fluxes (Table 2). The most notable change associated with the increase in pyruvate carboxylase activity was a 4-fold augmentation in the malic enzyme flux. This pathway, together with the pentose shunt, contributes to the formation of NADPH, a reducing agent needed for the synthesis of nucleotides and fatty acids. Interestingly, the amount of glucose channeled through the pentose phosphate pathway was reduced in the PYC-expressing cells, representing 7% of the glucose uptake rate, compared to 28% for the parental cells. However, the combined contribution of these two pathways towards NADPH formation remained relatively similar (2.3 and 2.5 pmol/cell d of NAPDH for the D9 and F5 cells, respectively). Although the catabolic rates of amino acids were individually small for both cell lines, these nutrients nonetheless account for a substantial portion of the total carbon entering the TCA cycle. Glutamine was the main amino acid consumed by the cells. Despite the observation of significant pyruvate recycling via the action of malic enzyme, the use of uniformly labeled substrate revealed that glutamine did not significantly contribute to lactate formation, due to its comparatively small uptake rate. This is not a universal finding, as glioblastoma cells were shown to metabolize 60% of glutamine to lactate (DeBerardinis et al., 2007), human diploid fibroblasts about 13% (Zielke et al., 1980) and hybridoma cells approximately 9% (Petch and Butler, 1994).

Other than the changes observed in the intracellular flux distribution, one of the key difference between the two clones lies in the reduced specific consumption rate of glucose by the PYC-expressing cells. Such behavior is normally observed in response to lower residual levels of glucose in the extracellular environment, but concentrations remained above 20 mM in all our cultures. The factors governing the glucose uptake cannot be inferred from the ^{13}C-metabolic flux analysis, but it can be speculated that some feedback mechanism is activated, presumably due to changes in the concentration of key intracellular metabolite pools resulting from the distinct metabolic flux distribution. Alternatively, an homeostatic mechanism may be reacting to variation in cofactors levels to maintain the redox potential (NAD^+/NADH ratio) or the energetic state of the cells (Neermann and Wagner, 1996; Zupke et al., 1995). Higher cell specific content of ATP have indeed been measured in PYC-expressing BHK cells (Irani et al., 1999). This regulation probably does not occur at the gene level, as gene expression profiling test using microarray analysis could not reveal any significant difference between the two cell clones (data not shown). Clearly, further work is needed to elucidate the mechanisms regulating substrate uptake in cultured mammalian cells.

5. Conclusion

The expression of PYC in HEK-293 cells was shown to enhance the yield of interferon-α2b production in batch culture, mainly through an augmentation in the integral of viable cell concentration. Isotopic labeling was employed to determine the metabolic flux distribution and demonstrated the presence of a significant pyruvate carboxylase activity that was missing in the parental clone. Such detailed analysis can provide invaluable information and constraints for further cellular engineering approaches, as well as guide the design of improved medium formulations and feeding strategies. The extension of culture times typically achieved in fed-batch cultures is usually associated with an increased cumulative glucose consumption and lactate accumulation. By delaying the accumulation of toxic waste metabolites, the favorable metabolism exhibited by the PYC-expressing HEK-293 cells make them particularly well-suited for employing concentrated nutrient solutions to further prolong the growth and/or production phases.

Acknowledgments

The authors wish to acknowledge the following contributors: Denise Boulais for isolating the 293-D9 and 293-F5 clones, Ping Hay Lam and Sabrina Yara for cell culture experiments, Louis Bisson for HPLC analysis and Jingkui Chen for ^{13}C LC/MS analysis

Appendix A

The biochemical reactions and the corresponding carbon atom transitions used for intracellular flux analysis (Table A1).

Table A1
Metabolic model and carbon atom transitions.

Glc_ext (abcdef)	→	G6P (abcdef)
G6P (abcdef)	→	F6P (abcdef)
G6P (abcdef)	→	R5P (bcdef)+CO (a)
R5P (abcde)+R5P (fghij)	→	S7P (abfghij)+G3P (cde)
R5P (abcde)+E4P (fghi)	→	F6P (abfghij)+G3P (cde)
S7P (abcdefg)+G3P (hij)	→	F6P (abchij)+E4P (defg)
F6P (abcdef)	→	G3P (cba)+G3P (def)
G3P (abc)	→	PYR (abc)
PYR (abc)	→	LAC_ext (abc)
PYR (abc)	→	ACCOA (bc)+CO (a)
PYR (abc)+CO (d)	→	OAA (abcd)
ACCOA (ab)+OAA (cdef)	→	CIT (fedbac)
CIT (abcdef)	→	AKG (abcde)+CO (f)
AKG (abcde)	→	MAL(½bcde+½edcb)+CO (a)
MAL (abcd)	→	OAA (abcd)
MAL (abcd)	→	PYR (abc)+CO (d)
PYR (abc)+GLU (defgh)	→	ALA (abc)+AKG (defgh)
GLU (abcde)	→	AKG (abcde)
CIT (abcdef)	→	LIPIDS+OAA (fcba)
Amino acids (Tyr, Leu, Ile, Lys, Phe)	→	ACCOA (ab)
Amino Acids (Val, Met, Ile, Thr)	→	MAL (abcd)
Amino Acids (Ser, Gly, Cys)	→	PYR (abc)
Amino Acids (Asp, Asn)	→	OAA (abcd)
R5P (abcde)	→	DNA/RNA
CO (a)	→	CO_ext (a)

References

Altamirano, C., et al., 2000. Improvement of CHO cell culture medium formulation: simultaneous substitution of glucose and glutamine. Biotechnol. Prog. 16, 69–75.

Altamirano, C., et al., 2004. Strategies for fed-batch cultivation of t-PA producing CHO cells: substitution of glucose and glutamine and rational design of culture medium. J. Biotechnol. 110, 171–179.

Andersen, D.C., Goochee, C.F., 1995. The effect of ammonia on the O-linked glycosylation of granulocyte colony-stimulating factor produced by chinese hamster ovary cells. Biotechnol. Bioeng. 47, 96–105.

Antoniewicz, M.R., et al., 2006. Determination of confidence intervals of metabolic fluxes estimated from stable isotope measurements. Metab. Eng. 8, 324–337.

Bebbington, C.R., et al., 1992. High-level expression of a recombinant antibody from myeloma cells using a glutamine synthetase gene as an amplifiable selectable marker. Biotechnology (N Y) 10, 169–175.

Birch, J.R., et al., 1994. Selecting and designing cell lines for improved physiological characteristics. Cytotechnology 15, 11–16.

Bonarius, H.P.J., et al., 2001. Metabolic-flux analysis of continuously cultured hybridoma cells using13-CO_2 mass spectrometry in combination with ^{13}C-lactate nuclear magnetic resonance spectroscopy and metabolite balancing. Biotechnol. Bioeng. 74, 528–538.

Borys, M.C., et al., 1994. Ammonia affects the glycosylation patterns of recombinant mouse placental lactogen-I by chinese hamster ovary cells in a pH-dependent manner. Biotechnol. Bioeng. 43, 505–514.

Brose, D.J., van Eikeren, P., 1990. A membrane-based method for removal of toxic ammonia from mammalian-cell culture. Appl. Biochem. Biotechnol. 24–25, 457–468.

Broussau, S., et al., 2008. Inducible packaging cells for large-scale production of lentiviral vectors in serum-free suspension culture. Mol. Ther. 16, 500–507.

Chang, Y.H., et al., 1995. In-situ removal of ammonium and lactate through electrical means for hybridoma cultures. Biotechnol. Bioeng. 47, 308–318.

Chen, K., et al., 2001. Engineering of a mammalian cell line for reduction of lactate formation and high monoclonal antibody production. Biotechnol. Bioeng. 72, 55–61.

Chen, P., Harcum, S.W., 2006. Effects of elevated ammonium on glycosylation gene expression in CHO cells. Metab. Eng. 8, 123–132.

Cockett, M.I., et al., 1990. High level expression of tissue inhibitor of metalloproteinases in Chinese hamster ovary cells using glutamine synthetase gene amplification. Biotechnology (N Y) 8, 662–667.

Cruz, H.J., et al., 2000. Effects of ammonia and lactate on growth, metabolism, and productivity of BHK cells. Enzyme Microb. Technol. 27, 43–52.

DeBerardinis, R.J., et al., 2007. Beyond aerobic glycolysis: transformed cells can engage in glutamine metabolism that exceeds the requirement for protein and nucleotide synthesis. Proc. Natl. Acad. Sci. USA 104, 19345–19350.

Deshpande, R., et al., 2009. Towards a metabolic and isotopic steady state in CHO batch cultures for reliable isotope-based metabolic profiling. Biotechnol. J. 4, 247–263.

Durocher, Y., Butler, M., 2009. Expression systems for therapeutic glycoprotein production. Curr. Opin. Biotechnol. 20, 700–707.

Durocher, Y., et al., 2002. High-level and high-throughput recombinant protein production by transient transfection of suspension-growing human 293-EBNA1 cells. Nucleic Acids Res. 30, E9.

Durocher, Y., et al., 2007. Scalable serum-free production of recombinant adeno-associated virus type 2 by transfection of 293 suspension cells. J. Virol. Methods 144, 32–40.

Elias, C.B., et al., 2003. Improving glucose and glutamine metabolism of human HEK 293 and Trichoplusia ni insect cells engineered to express a cytosolic pyruvate carboxylase enzyme. Biotechnol. Prog. 19, 90–97.

Europa, A.F., et al., 2000. Multiple steady states with distinct cellular metabolism in continuous culture of mammalian cells. Biotechnol. Bioeng. 67, 25–34.

Fogolin, M.B., et al., 2004. Impact of temperature reduction and expression of yeast pyruvate carboxylase on hGM-CSF-producing CHO cells. J. Biotechnol. 109, 179–191.

Gambhir, A., et al., 1999. Alteration of cellular metabolism by consecutive fed-batch cultures of mammalian cells. J. Biosci. Bioeng. 87, 805–810.

Gawlitzek, M., et al., 1998. Ammonium ion and glucosamine dependent increases of oligosaccharide complexity in recombinant glycoproteins secreted from cultivated BHK-21 cells. Biotechnol. Bioeng. 57, 518–528.

Genzel, Y., et al., 2005. Substitution of glutamine by pyruvate to reduce ammonia formation and growth inhibition of mammalian cells. Biotechnol. Prog. 21, 58–69.

Ghani, K., et al., 2006. Retroviral vector production using suspension-adapted 293GPG cells in a 3 L acoustic filter-based perfusion bioreactor. Biotechnol. Bioeng 95, 653–660.

Glacken, M.W., 1986. Reduction of waste product excretion via nutrient control: possible strategies for maximizing product and cell yields on serum in cultures of hybridoma cells. Biotechnol. Bioeng. 28, 1376–1389.

Grammatikos, S.I., et al., 1998. Intracellular UDP-N-acetylhexosamine pool affects N-glycan complexity: a mechanism of ammonium action on protein glycosylation. Biotechnol. Prog. 14, 410–419.

Hassell, T., Butler, M., 1990. Adaptation to non-ammoniagenic medium and selective substrate feeding lead to enhanced yields in animal cell cultures. J. Cell Sci. 96 (Pt 3), 501–508.

Hassell, T., et al., 1991. Growth inhibition in animal cell culture. The effect of lactate and ammonia. Appl. Biochem. Biotechnol. 30, 29–41.

Henry, O., et al., 2008. Simpler noninstrumented batch and semicontinuous cultures provide mammalian cell kinetic data comparable to continuous and perfusion cultures. Biotechnol. Prog. 24, 921–931.

Henry, O., et al., 2005. Metabolic flux analysis of HEK-293 cells in perfusion cultures for the production of adenoviral vectors. Metab. Eng. 7, 467–476.

Hofmann, U., et al., 2008. Identification of metabolic fluxes in hepatic cells from transient 13C-labeling experiments: Part I. Experimental observations. Biotechnol. Bioeng. 100, 344–354.

Irani, N., et al., 2002. Expression of recombinant cytoplasmic yeast pyruvate carboxylase for the improvement of the production of human erythropoietin by recombinant BHK-21 cells. J. Biotechnol. 93, 269–282.

Irani, N., et al., 1999. Improvement of the primary metabolism of cell cultures by introducing a new cytoplasmic pyruvate carboxylase reaction. Biotechnol. Bioeng. 66, 238–246.

Kamen, A., Henry, O., 2004. Development and optimization of an adenovirus production process. J. Gene. Med. 6 (Suppl 1), S184–S192.

Kim, S.H., Lee, G.M., 2007. Functional expression of human pyruvate carboxylase for reduced lactic acid formation of Chinese hamster ovary cells (DG44). Appl. Microbiol. Biotechnol. 76, 659–665.

Kurano, N., et al., 1990. Growth behavior of Chinese hamster ovary cells in a compact loop bioreactor. 2. Effects of medium components and waste products. J. Biotechnol. 15, 113–128.

Kurokawa, H., et al., 1994. Growth Characteristics in Fed-Batch Culture of Hybridoma Cells with Control of Glucose and Glutamine Concentrations. Biotechnol. Bioeng. 44, 95–103.

Lee, Y.Y., et al., 2003. Low-glutamine fed-batch cultures of 293-HEK serum-free suspension cells for adenovirus production. Biotechnol. Prog. 19, 501–509.

Lioussanne, L., et al., 2008. Mycorrhizal colonization with Glomus intraradices and development stage of transformed tomato roots significantly modify the chemotactic response of zoospores of the pathogen Phytophthora nicotianae. Soil Biol. Biochem. 40, 2217–2224.

Ljunggren, J., Haggstrom, L., 1992. Glutamine limited fed-batch culture reduces the overflow metabolism of amino acids in myeloma cells. Cytotechnology 8, 45–56.

Ljunggren, J., Haggstrom, L., 1994. Catabolic control of hybridoma cells by glucose and glutamine limited fed batch cultures. Biotechnol. Bioeng. 44, 808–818.

Loignon, M., et al., 2008. Stable high volumetric production of glycosylated human recombinant IFNalpha2b in HEK293 cells. BMC Biotechnol. 8, 65.

Luan, Y.T., et al., 1987. Effect of various glucose/glutamine ratios on hybridoma growth, viability and monoclonal antibody formation. Cytotechnology 9, 535–538.

Mancuso, A., et al., 1994. Examination of primary metabolic pathways in a murine hybridoma with carbon-13 nuclear magnetic resonance spectroscopy. Biotechnol. Bioeng. 44, 563–585.

Metallo, C.M., et al., 2009. Evaluation of ^{13}C isotopic tracers for metabolic flux analysis in mammalian cells. J. Biotechnol. 144, 167–174.

Nadeau, I., et al., 2002. Low-protein medium affects the 293SF central metabolism during growth and infection with adenovirus. Biotechnol. Bioeng. 77, 91–104.

Nayve Jr., F.R., et al., 1991. Selective removal of ammonia from animal cell culture broth. Cytotechnology 6, 121–130.

Neermann, J., Wagner, R., 1996. Comparative analysis of glucose and glutamine metabolism in transformed mammalian cell lines, insect and primary liver cells. J. Cell. Physiol. 166, 152–169.

Please cite this article as: Henry, O., Durocher, Y., Enhanced glycoprotein production in HEK-293 cells expressing pyruvate carboxylase. Metab. Eng. (2011), doi:10.1016/j.ymben.2011.05.004

Ng, S.K., et al., 2007. Application of destabilizing sequences on selection marker for improved recombinant protein productivity in CHO-DG44. Metab. Eng. 9, 304–316.

Omasa, T., et al., 2009. Enhanced antibody production following intermediate addition based on flux analysis in mammalian cell continuous culture. Bioprocess Biosyst. Eng. 33, 117–125.

Omasa, T., et al., 1992a. Effects of lactate concentration on hybridoma culture in lactate-controlled fed-batch operation. Biotechnol. Bioeng. 39, 55–564.

Omasa, T., et al., 1992b. The enhancement of specific antibody production rate in glucose and glutamine controlled fed-batch culture. Cytotechnology 8, 75–84.

Ozturk, S.S., et al., 1992. Effects of ammonia and lactate on hybridoma growth, metabolism, and antibody production. Biotechnol. Bioeng. 39, 418–431.

Peng, R.W., et al., 2010. The vesicle-trafficking protein munc18b increases the secretory capacity of mammalian cells. Metab. Eng. 12, 18–25.

Petch, D., Butler, M., 1994. Profile of energy metabolism in a murine hybridoma: glucose and glutamine utilization. J. Cell. Physiol. 161, 71–76.

Pham, P.L., et al., 2003. Large-scale transient transfection of serum-free suspension-growing HEK293 EBNA1 cells: peptone additives improve cell growth and transfection efficiency. Biotechnol. Bioeng. 84, 332–342.

Quek, L.E., et al., 2009a. Metabolic flux analysis in mammalian cell culture. Metab. Eng. 12, 161–172.

Quek, L.E., et al., 2009b. OpenFLUX: efficient modelling software for ^{13}C-based metabolic flux analysis. Microb. Cell Fact. 8, 25.

Siegwart, P., et al., 1999. Adaptive control at low glucose concentration of HEK-293 cell serum-free cultures. Biotechnol. Prog. 15, 608–616.

Wurm, F.M., 2004. Production of recombinant protein therapeutics in cultivated mammalian cells. Nat. Biotechnol. 22, 1393–1398.

Xie, L., Wang, D.I.C., 1996. High cell density and high monoclonal antibody production through medium design and rational control in a bioreactor. Biotechnol. Bioeng. 51, 725–729.

Zhang, P., et al., 2010. A functional analysis of N-glycosylation-related genes on sialylation of recombinant erythropoietin in six commonly used mammalian cell lines. Metab. Eng. 12, 526–536.

Zhou, W., et al., 1995. High viable cell concentration fed-batch cultures of hybridoma cells through on-line nutrient feeding. Biotechnol. Bioeng. 46, 579–587.

Zielke, H.R., et al., 1980. Lactate: a major product of glutamine metabolism by human diploid fibroblasts. J. Cell. Physiol. 104, 433–441.

Zupke, C., et al., 1995. Intracellular flux analysis applied to the effect of dissolved oxygen on hybridomas. Appl. Microbiol. Biotechnol. 44, 27–36.

Please cite this article as: Henry, O., Durocher, Y., Enhanced glycoprotein production in HEK-293 cells expressing pyruvate carboxylase. Metab. Eng. (2011), doi:10.1016/j.ymben.2011.05.004